

Low-Temperature Synthesis, Structure, and Stability of $\text{Ba}_{2+y}\text{Cu}_3\text{O}_6$

Eric L. Brosha,¹ Fernando H. Garzon, and Ian D. Raistrick

Los Alamos National Laboratory, Los Alamos, New Mexico 87545

and

Peter K. Davies

Department of Materials Science and Engineering, University of Pennsylvania, Philadelphia, Pennsylvania 19104-6272

Received August 1, 1995; in revised form December 11, 1995; accepted December 14, 1995

Single-phase powders of $\text{Ba}_2\text{Cu}_3\text{O}_6$ have been prepared at 620°C under 1 atm of oxygen using freeze-dried nitrate precursors. Calcinations utilizing a precursor with a 1:1 Ba:Cu stoichiometry produced a two-phase mixture of $\text{BaO}_2 + \text{Ba}_2\text{Cu}_3\text{O}_6$ and confirmed the stable, oxidized barium cuprate exists with a metal ion ratio close to 2:3. Diffraction studies suggest that $\text{Ba}_2\text{Cu}_3\text{O}_6$ ($\text{Ba}_{0.67}\text{CuO}_2$) crystallizes in a structure closely related to the linear chain KCuO_2 and NaCuO_2 cuprates. It is proposed that the reduction of copper and accompanying loss of oxygen observed above 620°C are accommodated by an increase in the Ba content of the structure and the formation of $\text{Ba}_{2+y}\text{Cu}_3\text{O}_6$ with $0 \leq y \leq 0.25$. Above 710°C, the high- y end member is metastable with respect to BaCuO_2 , although it decomposes slowly even at elevated temperatures. © 1996 Academic Press, Inc.

I. INTRODUCTION

All of the high- T_c superconductors in the Y–Ba–Cu–O system have been shown to be metastable at low temperatures under 1 atm of oxygen (1–8). Low-temperature phase studies at the Y:Ba:Cu = 1:2:4 composition conducted using freeze-dried nitrate precursors (1) indicated that below 675°C the stable phase assemblage is Y_2O_3 , CuO, and an oxidized, semiconducting barium cuprate, $\text{Ba}_2\text{Cu}_3\text{O}_6$. This result was later confirmed using high-precision perchloric acid solution calorimetry (2). The dominant stability of $\text{Ba}_2\text{Cu}_3\text{O}_6$ at low temperatures under oxygen is directly related to the valence of Cu (+2.66), which is the highest of any cuprate in the Y–Ba–Cu–O system. Several conflicting reports have appeared in the literature regarding the stoichiometry, structure, and stability of $\text{Ba}_2\text{Cu}_3\text{O}_6$. In many cases these contradictions have arisen from the difficulty in preparing single-phase, BaCO_3 -free samples and the apparent incommensurate modulation of the bar-

ium ion positions within the structure. In this paper we report on our own studies of the composition, phase homogeneity, structure, and stability of $\text{Ba}_2\text{Cu}_3\text{O}_6$ which was synthesized at low temperature under 1 atm of oxygen using a freeze-dried nitrate precursor route. While we were unable to improve upon previous refinements of the structure (9, 10), we believe our results resolve the confusion surrounding the stoichiometry, crystal chemistry, and thermal stability of $\text{Ba}_2\text{Cu}_3\text{O}_6$.

The existence of an oxidized binary cuprate with a Ba:Cu concentration close to 2:3 was first reported by Halasz *et al.* (11) and subsequently investigated in detail by Thompson *et al.* (9, 10). By reacting BaO_2 and CuO at 680°C under overpressures of oxygen ranging from 10 to 15 atm, Thompson obtained samples of “ $\text{Ba}_2\text{Cu}_3\text{O}_{5+\delta}$ ” with $0.5 \leq \delta \leq 0.9$. Similar results were reported by Williams *et al.* (12), who obtained samples with a larger grain size using a high temperature (980°C), high p_{O_2} (58 bar) route. While these and other investigations of the low-temperature phase equilibria in the Ba–Cu–O system (13, 14) support the formation of an oxidized barium cuprate with a 2:3 Ba:Cu stoichiometry, reports on the preparation of a trivalent cuprate, $\text{BaCuO}_{2.5}$, with a 1:1 stoichiometry have consistently appeared in the literature over the past 20 years (15–18).

As noted by Thompson *et al.* (9, 10) and Roth (13), the X-ray patterns in the first paper on the preparation of “ $\text{BaCuO}_{2.5}$ ” (15) were mistakenly interpreted in terms of a single-phase product, and can be indexed to a two-phase mixture of $\text{Ba}_2\text{Cu}_3\text{O}_6$ and BaCO_3 . Despite this corrected interpretation, three other reports have recently appeared on the preparation of $\text{BaCuO}_{2.5}$. Machida *et al.* (16) reacted equimolar mixtures of $\text{Ba}(\text{NO}_3)_2$ and $\text{Cu}(\text{NO}_3)_2$ in air and claimed single-phase samples of $\text{BaCuO}_{2.5}$ were formed at 650°C. However, their x-ray patterns are essentially identical to those collected by Arjomand and Machin (15) and

¹ To whom correspondence should be addressed.

again can be indexed in terms of a BaCO₃ + Ba₂Cu₃O₆ two-phase mixture. Petricek *et al.* (17) also reported that 1:1 mixtures of BaO₂ and CuO yield a single-phase BaCuO_{2+x} product at 540 and 560°C under a p_{O_2} of 90 and 385 kPa, respectively. In that work, the BaO₂ precursor was purified to exclude any BaCO₃ and correspondingly the listed d -spacings, which were interpreted in terms of a single-phase BaCuO_{2.5} product, show no evidence for carbonate formation. With the exception of several additional lines, the strongest of which have d -spacings = 6.419, 4.701, 2.587, 2.400, 2.323 Å, the X-ray patterns quoted by Petricek *et al.* (17) are identical to those reported for Ba₂Cu₃O₆ (9, 10). However, these additional reflections correspond to a second phase of Ba(OH)₂·H₂O which presumably formed because of the presence of H₂O in the reaction system. Noting the results in (9, 10), Petricek *et al.* repeated their synthesis using a BaO₂:CuO mole ratio of 2:3. Although they report the final product contained “BaCuO_{2.5}” and excess CuO, we suggest this preparation actually failed to come to completion and yielded a mixture of Ba₂Cu₃O₆ + Ba(OH)₂·H₂O + CuO. The most recent report on the formation of BaCuO_{2.5} was made by Mingmei *et al.* (18), who reacted an equimolar mixture of BaO₂ and CuO under an oxygen gas flow at 550°C for 60 h. However, careful inspection of their X-ray data shows reflections from Ba₂Cu₃O₆ plus strong additional lines that correspond to BaO₂ and BaCO₃.

While the difficulty in achieving equilibrium and avoiding carbonate formation has contributed to the contradictions in the literature, the debate surrounding the composition and crystal chemistry of Ba₂Cu₃O₆ has also been complicated by the apparent incommensurate nature of its structure and by the possible existence of several different polymorphs. Using electron and X-ray diffraction Thompson *et al.* (9, 10) concluded that “Ba₂Cu₃O_{5+δ}” has an incommensurate, vernier-type structure with infinite chains of edge-shared CuO₄ square planes separated by a layered Ba sublattice. In addition to finding that the structure modulation was sensitive to the oxygen content, evidence was provided for at least three different, though related forms of the 2:3 barium cuprate phase. The first was a “low-ordered” form stable below 700°C with $\delta = 1$ (i.e., Ba₂Cu₃O₆); this structure was modeled using a monoclinic supercell in which the linear CuO₂ chains are interspersed by a hexagonal Ba sublattice. Below 700°C for $1.0 > \delta > 0.0$, a “low-disordered” form of Ba₂Cu₃O_{5+δ} was formed with a structure claimed to be based on a primitive hexagonal Ba array and a CuO₂ sublattice consisting of short chains randomly oriented in three directions. A third “high-disordered” form of Ba₂Cu₃O_{5+δ} was also reported to exist above 700°C for $\delta < 0.5$. The transitions between the various structures were apparently driven by the changes in the bulk oxygen content, and, therefore, in the formal copper valence.

II. EXPERIMENTAL

The samples of Ba₂Cu₃O₆ studied in this work were prepared by an ultrasonic, freeze-dried nitrate technique. A detailed description of the techniques is presented in Ref. (1) and only a summary is given here. Stoichiometric quantities of CuO and Ba(NO₃)₂ were dissolved in deionized/distilled water with the aid of dilute nitric acid and heat. The solutions were stirred until all traces of the oxides had disappeared and then passed through an ultrasonic atomizer (Sono-Tek) to form micrometer-sized droplets. The droplets were rapidly frozen in liquid nitrogen to preserve the intimate mixing of the solution state. After removing the solvent via sublimation at reduced temperatures and pressures in a commercial freeze-dryer, a highly reactive precursor was obtained for subsequent studies of the low-temperature solid-state phase equilibria.

Two precursors with Ba:Cu = 2:3 and 1:1 were investigated. They were placed into platinum or gold foil boats, depending on the annealing temperature, and plunged into a preheated tube furnace under 1 atm of flowing oxygen. The decomposition of the nitrate precursor was accompanied by a rapid evolution of NO₂ and water vapor. Although the reactions of the freeze-dried precursors generally occurred within minutes, the samples were usually annealed for 18 to 20 h to improve their crystallinity. All of the powders were characterized using a Seimens D5000 powder X-ray diffractometer (XRD) that utilizes CuK_α radiation. Thermogravimetric analysis was performed using a Perkin/Elmer TGA-7.

III. RESULTS AND DISCUSSION

A. Stoichiometry

As discussed in the Introduction, there has been considerable debate over the existence and exact stoichiometry of a copper-rich barium cuprate. Much of this discussion has focussed on the conflicting reports of an oxidized 1:1 cuprate with a stoichiometry approaching BaCuO_{2.5} versus a 2:3 cuprate generally described as Ba₂Cu₃O_{5+δ} (or Ba₂Cu₃O_{6-x}). The disagreements have largely arisen due to the failure to recognize the formation of second phases of BaCO₃ and BaO₂ which are potentially stable phases under the low temperature, high p_{O_2} conditions employed during the sample synthesis. Therefore, our first objective was to resolve this controversy and to demonstrate that the oxidized barium cuprate that is formed in this region of the phase diagram is indeed copper-rich. To this end, a freeze-dried nitrate precursor was prepared with Ba:Cu = 1:1. A portion of the sample was reacted at 900°C for 18 h under flowing oxygen. The X-ray patterns only contained reflections from the divalent cuprate BaCuO₂, see Figure 1a. Another portion of the 1:1 precursor was reacted at 620°C under pure oxygen, after 18 h of heating this pattern

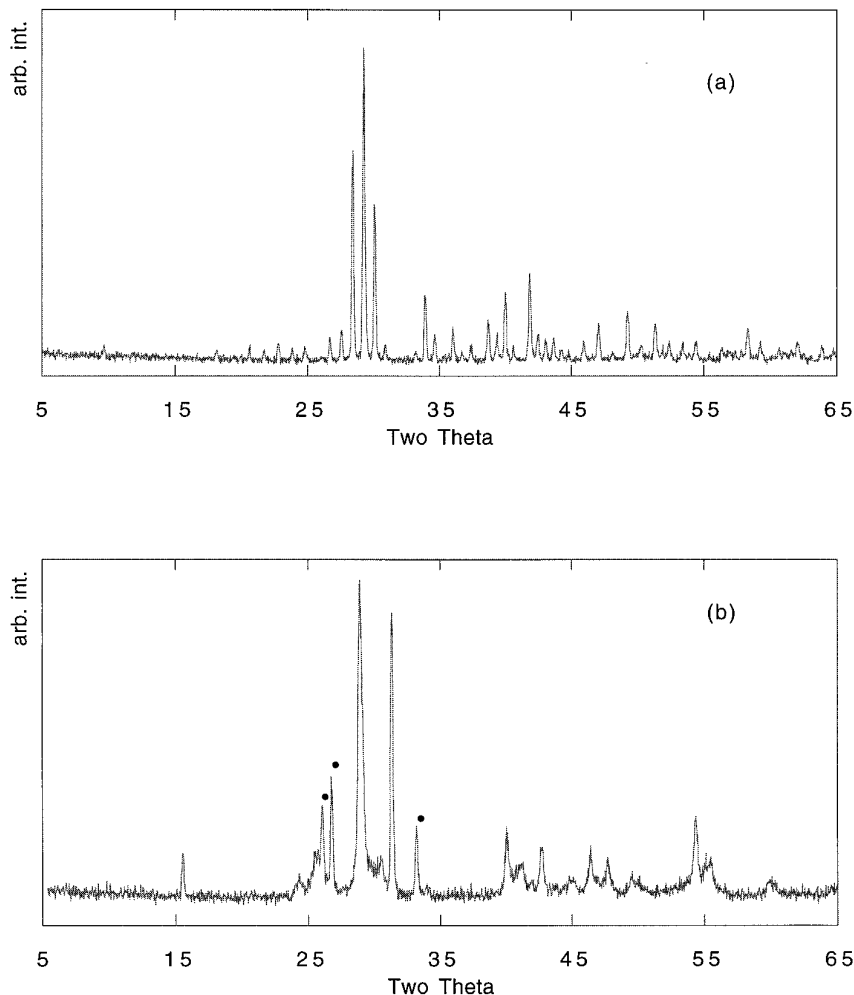


FIG. 1. X-ray patterns collected from a freeze-dried nitrate precursor with Ba:Cu = 1:1 after reaction under 1 atm of oxygen at (a) 900°C and (b) 620°C. Principle BaO₂ peaks are indicated (•).

(Fig. 1b) contains reflections from BaO₂ and the Ba₂Cu₃O_{5+δ} phase reported by Thompson *et al.* (9, 10). This result is in direct conflict with the claims of a stable oxidized cuprate with a 1:1 stoichiometry and supports the existence of a copper-rich phase at low temperature in which the Ba and Cu are present in a 2:3 ratio. The observation of a second phase of BaO₂ agrees with the phase equilibria studies of Roth (13) and suggests that the barium-rich cuprate Ba₂CuO₃, which is known to exist at higher temperature, is also unstable in the 600–650°C range. We did not make any further attempts to characterize the lower temperature stability limit of Ba₂CuO₃.

Preparation of single-phase samples of Ba₂Cu₃O₆ was accomplished through reactions of freeze-dried nitrate precursors with Ba:Cu = 2:3. The reflections in the X-ray patterns collected from a powder reacted at 620°C under a flow of oxygen gas, Fig. 2, were in agreement with those reported previously (9, 10). A weak reflection observed in

the patterns at $2\theta = 23.9^\circ$ could correspond to trace amounts of BaCO₃, though it is possible that this may originate from the modulations within the Ba₂Cu₃O₆ structure. The d-spacings and relative intensities are reported in Table 1. The oxygen content listed in the formula was in agreement with the results of TGA analyses using forming gas.

B. Structure

Although the similarity between the two structures has not been noted previously, the models proposed by Thompson *et al.* (9, 10) indicate that the low-temperature form of Ba₂Cu₃O_{5+δ} with $\delta = 1$, is closely related to the structure of the alkali cuprates ACuO₂ (A = Na, K, Cs, Rb). These structures all contain infinite, one-dimensional chains of edge-shared square-planar cuprate groups cross-linked by the larger electropositive cations (19). In the

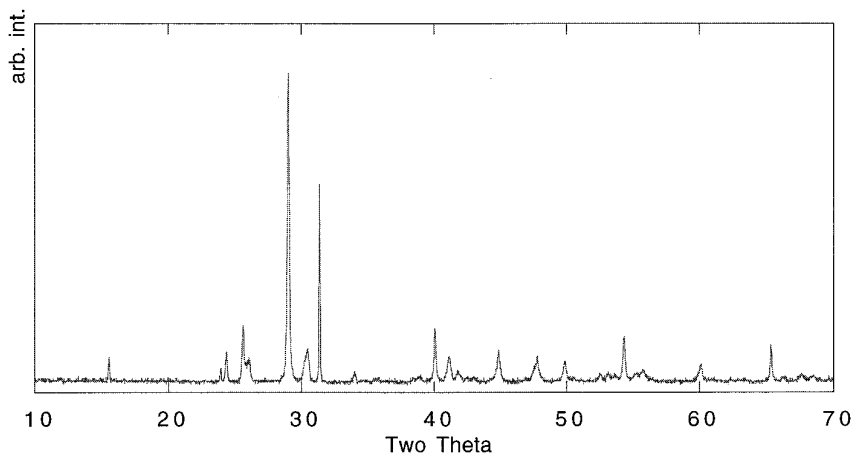


FIG. 2. X-ray pattern of $\text{Ba}_2\text{Cu}_3\text{O}_6$ sample prepared at 620°C under pure oxygen.

NaCuO_2 -type phases, the copper atoms at the centers of the CuO_4 planar groups in the CuO_2 sublattice adopt a face-centered orthorhombic arrangement with, using the setting adopted in recent studies, the linear chains parallel to the a -axis; see Fig. 3 (20–24). For NaCuO_2 , which actu-

ally undergoes a very small monoclinic distortion from orthorhombic symmetry, the cross-linking Na atoms occupy octahedral sites in the interchain channels (21–23). This structure is also adopted in the low-temperature form of calcium cuprate, Ca_xCuO_2 ($x = 0.8\text{--}0.85$) (21, 24), and by several ternary calcium-rare earth cuprates, $(\text{Ca}_{2-x}\text{RE}_{2+x})\text{Cu}_5\text{O}_{10} - \text{RE} = \text{Y, Gd, Nd}$ (20, 25). In the nonstoichiometric $A_{1-x}\text{CuO}_2$ phases the reduced occupancy of the interchain sites leads to variable incommensurability arising from a mutual modulation of the A and Cu sublattices. The A ions were shown to be located on a C-centered monoclinic or orthorhombic sublattice, with the Cu sublatt-

TABLE 1
Indexing Scheme for Ba Subcell in $\text{Ba}_2\text{Cu}_3\text{O}_6$

$2\theta_{\text{obs}}$	$2\theta_{\text{calc}}$	I_{rel}	h	k	l
15.54	15.52	8	0	0	2
23.94	23.37	4	0	0	3
24.37	24.33	10	1	1	0
	24.34		0	2	0
25.61	25.57	19	1	1	1
26.03		7			
29.01	29.00	100	0	2	2
30.45		11			
31.36	31.33	65	0	0	4
34.01	33.99	4	1	1	3
40.08	40.07	18	0	2	4
41.14		8			
41.84		3			
42.48		1			
42.97	42.82	1	1	3	0
44.20	44.12	1	0	3	3
44.87		10			
47.80	47.79	8	0	0	6
49.88	49.88	6	0	4	0
50.53	50.54	1	2	2	1
52.55	52.56	3	0	2	4
53.75	54.02	2	1	3	4
54.34	54.34	14	0	2	6
55.75	55.76	3	2	2	3
60.08	60.10	1	0	4	4
65.35	65.36	12	2	2	5
	65.37		0	0	8

Note. $a = 4.225(2)$, $b = 7.312(2)$, $c = 11.420(2)$ Å.

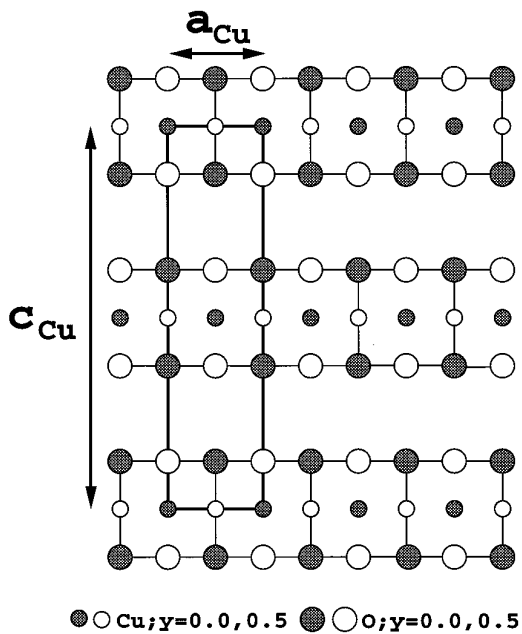


FIG. 3. Schematic [010] projection of the face-centered, orthorhombic CuO_2 sublattice in the NaCuO_2 -type structure.

tice retaining a fcc arrangement (20, 21, 24). Extensive investigations of the $\text{Ca}_{1-x}\text{CuO}_2$ (or $\text{Ca}_{5+x}\text{Cu}_6\text{O}_{12}$) system using high-resolution TEM (24) and the ternary ($\text{Ca}_{2-x}\text{RE}_{2+x}$) Cu_5O_{10} cuprates using X-ray and electron diffraction (20) have shown that the modulations in these systems are quite complicated and vary according to the chemistry and concentration of the *A*-site ions in the interchain positions.

In the KCuO_2 structure (22, 26), the linear cuprate chains are displaced by half a polyhedron to remove the centering of the Cu sublattice in the (001) plane (using the setting adopted above for NaCuO_2), and the larger alkali ions [K, Cs (27), Rb (28)] occupy uncapped trigonal prismatic sites. There are no reports of other phases with this type of chain arrangement. In the related MAuO_2 phases, e.g. KAuO_2 , the Cu atoms adopt a primitive sub-lattice and the CuO_2 chains are linked by cubic polyhedra (28).

The key crystallographic features of $\text{Ba}_2\text{Cu}_3\text{O}_6$, or $\text{Ba}_{0.67}\text{CuO}_2$, reported by Thompson *et al.* (9, 10) bear a marked resemblance to those identified above for the ACuO_2 structures. While complete refinement was not accomplished, due in part to the complex modulations and the poor crystallinity, it was concluded that the barium ions in $\text{Ba}_2\text{Cu}_3\text{O}_6$ are located on a *C*-centered orthorhombic lattice and a primitive, monoclinic CuO_2 sublattice was comprised of linear chains of edge-shared CuO_4 square planes. A commensurate model for the superstructure was proposed using a monoclinic lattice with $a = 8.48 \text{ \AA}$, $b = 7.33 \text{ \AA}$, $c = 12.15 \text{ \AA}$, $\beta = 110.4^\circ$; see Fig. 4 (10).

While the models proposed for the structure of $\text{Ba}_2\text{Cu}_3\text{O}_6$ are in reasonable agreement with the experimental X-ray patterns some reflections, for example at $2\theta = 30.45$, presumed to arise from the mutual modulation of the two sublattices could not be indexed. During our own investigations of this system we made many attempts to improve upon these models but had no significant success. However, we believe our interpretation of this system in terms of the formation of an ACuO_2 -type lattice does provide some new insights into the crystal chemistry and stability of $\text{Ba}_2\text{Cu}_3\text{O}_6$.

The positions of most of the reflections in our X-ray patterns (Fig. 2) of $\text{Ba}_2\text{Cu}_3\text{O}_6$ could be indexed using the *C*-centered orthorhombic cell proposed for the Ba sublattice (9, 10). Using the indexing scheme shown in Table 1, these refined to a cell with $a_{\text{Ba}} = 4.225(2) \text{ \AA}$, $b_{\text{Ba}} = 7.312(2) \text{ \AA}$, and $c_{\text{Ba}} = 11.420(2) \text{ \AA}$, which is in good agreement with the previously reported values. In this cell, the repeat along the *a* direction corresponds to one Ba–Ba separation. A “composite” ACuO_2 -type supercell can then be constructed for $\text{Ba}_2\text{Cu}_3\text{O}_6$ by adding a primitive monoclinic CuO_2 sublattice, with a_{Cu} corresponding to one Cu–Cu separation, b_{Cu} equal to and coincident with the Ba sublattice, and $2c_{\text{Cu}} = c_{\text{Ba}}/\sin \beta$ where $\tan \beta = -(c_{\text{Ba}}/a_{\text{Ba}})$; see Fig. 4. In the resultant monoclinic supercell, where $a =$

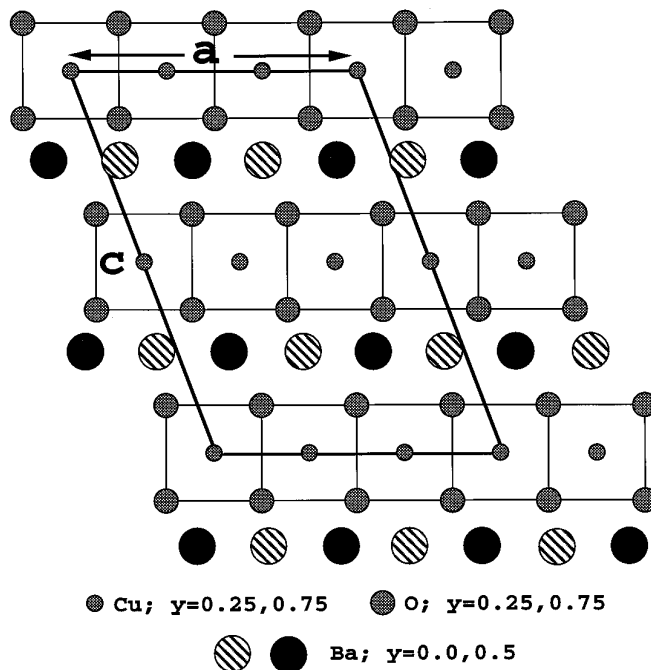


FIG. 4. Projection onto (010) of the monoclinic supercell proposed for $\text{Ba}_2\text{Cu}_3\text{O}_6$ in (10).

8.450 \AA , $b = 7.312 \text{ \AA}$, $c = 12.176 \text{ \AA}$, and $\beta = 110.3^\circ$, the repeat distance along *a* corresponds to the smallest common multiple of the Ba–Ba and Cu–Cu repeats in the two subcells, i.e., $a_{\text{super}} = 2a_{\text{Ba}} = 3a_{\text{Cu}}$. The *a* repeat of the Cu subcell in $\text{Ba}_2\text{Cu}_3\text{O}_6$, 2.817 \AA , is essentially identical to those observed in the $\text{Ca}_{1-x}\text{CuO}_2$ (2.807 \AA) and $\text{Ca}_{2+x}\text{M}_{2-x}\text{Cu}_5\text{O}_{10}$ ($2.811\text{--}2.833 \text{ \AA}$) phases (20, 21, 24). As expected the volume of the supercell for the barium cuprate, $V_{\text{Ba}_{0.67}\text{CuO}_2} = 705.6/3 = 235.2 \text{ \AA}^3$, is larger than that of the calcium isomorph, $V_{\text{Ca}_{0.8}\text{CuO}_2} = 189 \text{ \AA}^3$.

The formation of a primitive, monoclinically distorted Cu sublattice implies that $\text{Ba}_2\text{Cu}_3\text{O}_6$ is more closely related to the KCuO_2 -type rather than NaCuO_2 -type structure. However, consideration of the *b*-axis cell repeats of the different linear-chain cuprates, which are particularly sensitive to the *C*-centering and the size and coordination of the *A*-site cations, point to a similarity to NaCuO_2 . In Fig. 5, we show data for the cell repeats along this direction of the lattice plotted as a function of the radius of the six-coordinated *A*-site cation for the known NaCuO_2 and KCuO_2 phases. For the *C*-centered NaCuO_2 structures data is included for the Na, Ca, and Ca–*RE* isomorphs; for the KCuO_2 -type sublattice this direction corresponds to the *a* repeat in the settings used for the K, Cs, and Rb isomorphs in Refs. (22, 27, 28). Note that for meaningful comparison of the centered and primitive arrangement of the Cu atoms in this plane, $2a_{\text{KCuO}_2}$ is used in Fig. 5.

In both structure types an excellent correlation is found

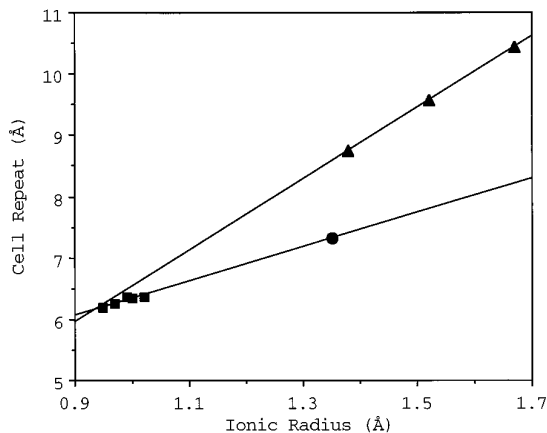


FIG. 5. Cell repeat as a function of the six-coordinate ionic radius of the cross-linking channel cations for (a) b -axis of NaCuO₂-type structures (squares) and (b) $2a$ for KCuO₂-type structures (triangles). Filled circle corresponds to b for Ba₂Cu₃O₆; see text.

between the lattice dimension and the ionic radius of the A -site ion. As expected the removal of the centering, which is also associated with in the change in coordination of the A -site ions from octahedral to triangular prismatic, is reflected by a significant relative increase in the lattice dimension of the KCuO₂ phases. The b -parameter obtained from the refinements of Ba₂Cu₃O₆ lies on the trend expected the NaCuO₂-type, Cu sublattice.

To summarize, although we have been unable to improve upon the structure refinements of Ba₂Cu₃O₆ reported in (9, 10), the crystal chemistry of this system has been reinterpreted in terms of the formation of an NaCuO₂/KCuO₂-type structure. The structure refinements support the formation of a monoclinic Cu sublattice, while the lattice parameters point to similarities to the NaCuO₂-type phases. In practice the structure of Ba₂Cu₃O₆ is incommensurately modulated and considerable uncertainty remains as to the exact details of the local coordination polyhedra.

In a structure based on an edge-shared arrangement of CuO₄ square-planes, it is perhaps difficult to reconcile the “nondestructive” loss of oxygen observed when Ba₂Cu₃O₆ is heated above 650°C. Elimination of oxygen and retention of an ACuO₂-type lattice without any additional compositional changes would clearly lead to the unreasonable conclusion that some of the copper ions adopt threefold coordination. In the following section, we examine the thermal stability of Ba₂Cu₃O₆ and the mechanism for the elimination of oxygen from the structure.

C. Thermal Stability and Oxygen Loss

The thermogravimetric response of samples of Ba₂Cu₃O₆ prepared at 620°C is shown in Fig. 6. Three major regions of weight loss were observed; the first corresponds

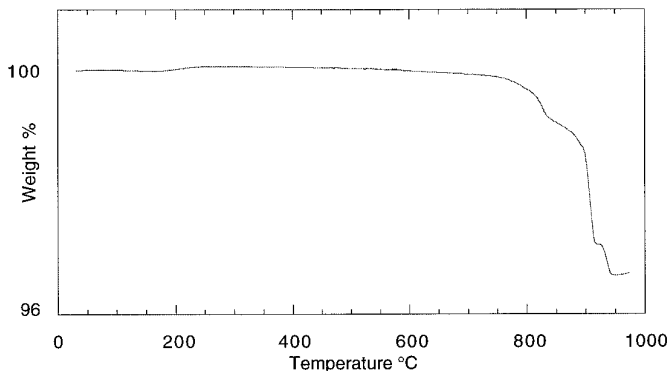
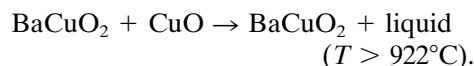
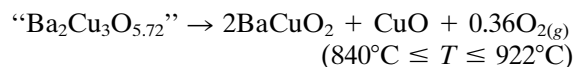
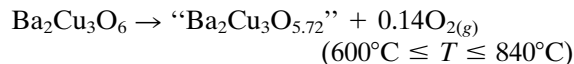


FIG. 6. TGA (10°C/min under O₂ flow) of a Ba₂Cu₃O₆ sample prepared at 620°C and $p_{O_2} = 1$ atm.

to the variable oxygen stoichiometry reported by Thompson *et al.* for Ba₂Cu₃O_{5+ δ} (9) and occurs over a range of temperature beginning at 650°C. The more abrupt weight loss at 840°C is due to bulk decomposition, while the final loss at 900°C is the result of partial melting (29). Quantification of the weight losses yields the following sequence of decompositions:



More detailed investigations of the path of the reduction reaction were made by directly reacting several samples of the freeze-dried Ba₂Cu₃O₆ precursor under reduced oxygen pressures. The first sample was annealed at 620°C in a gas flow with $p_{O_2} = 0.01$ atm. The X-ray patterns were similar to those collected from samples prepared in a $p_{O_2} = 1$ atm, but with slight shifts in some of the peak positions. Similar patterns were also obtained from samples prepared at 500°C under flowing argon with $p_{O_2} = 10^{-3}$ atm; see Fig. 7. Thermogravimetric analyses of this sample under forming gas were consistent with a stoichiometry Ba₂Cu₃O_{5.62}. As reported in (9, 10), the reflections exhibiting the largest shifts in the samples with a reduced oxygen content were those presumed to originate from the mutual modulation of the Ba and Cu subcells. The peak broadening and poor crystallinity associated with the reduced synthesis temperature precluded any detailed structural analysis. The stronger peaks in the pattern, primarily (00 l) and (0 kl) reflections could be fitted to an orthorhombic cell with, $a = 4.21$ Å, $b = 7.27$ Å, $c = 11.43$ Å, but the fit, particularly of a , must be treated with caution.

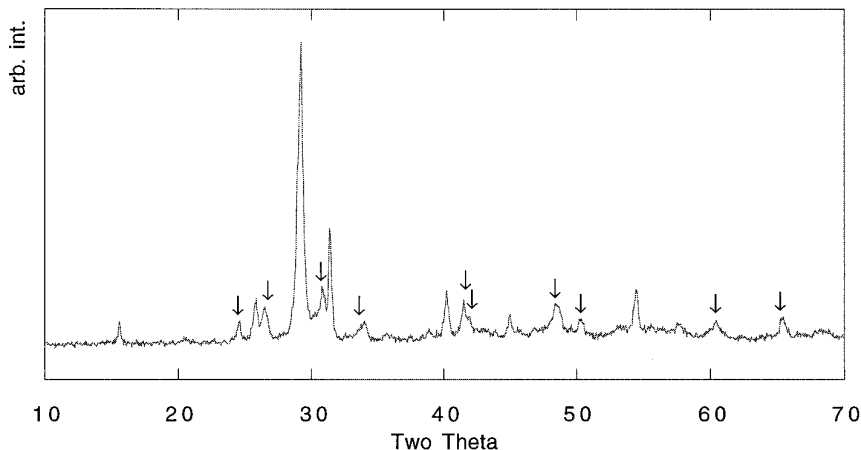
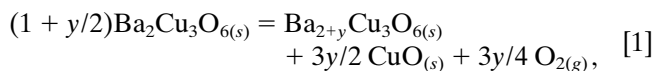
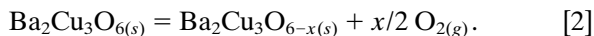


FIG. 7. X-ray pattern of $\text{Ba}_2\text{Cu}_3\text{O}_{6-x}$ prepared at 500°C at $p_{\text{O}_2} = 10^{-3}$ atm. Arrows indicate peaks showing largest shifts or broadening as compared to $p_{\text{O}_2} = 1$ atm preparations.

In accordance with the previous studies, the results presented above confirm that oxygen can be eliminated from $\text{Ba}_2\text{Cu}_3\text{O}_6$ without inducing complete decomposition of the structure. However, to reconcile these results with the fixed oxygen stoichiometry of the ACuO_2 -type lattice proposed above, we propose that the reduction of copper in $\text{Ba}_2\text{Cu}_3\text{O}_6$ is accommodated by small adjustments in the Ba:Cu stoichiometry and formation of $\text{Ba}_{2+y}\text{Cu}_3\text{O}_6$ rather than $\text{Ba}_2\text{Cu}_3\text{O}_{6-x}$. Using this model the reduction reaction can be written as



which should be contrasted to the existing models where



In this model, the reduction of $\text{Ba}_2\text{Cu}_3\text{O}_6$ results in a small increase in the concentration of Ba in the channels of the ACuO_2 -type structure and the formation of small amounts of second-phase CuO . The degree of reduction and the range of stoichiometry, y , in $\text{Ba}_{2+y}\text{Cu}_3\text{O}_6$ will be constrained by chemical and structural factors. Complete reduction of Cu to the +2 state would yield a phase with $y = 1$, while complete oxidation of Cu to the trivalent state would correspond to a phase with $y = -0.5$, i.e., $\text{Ba}_{1.5}\text{Cu}_3\text{O}_6$.

The oxidation thermodynamics of the Cu ion are certainly a key factor in determining the composition of this phase; however, structural factors, in particular the concentration of the Ba ions and therefore the Ba–Ba distances within the interchain channels, will also make a strong contribution to the overall stability. For negative values of y , significant depletions in the number of cross-linking

Ba ions in the channels would ultimately lead to elimination of the “structural integrity” of the system and complete collapse of the structure. Prior to the discovery of $\text{Ba}_2\text{Cu}_3\text{O}_6$, the lowest concentration of channel ions in an $\text{A}_{1-x}\text{CuO}_2$ sodium-cuprate-type structure was reported in $(\text{Nd}_2\text{Ca})\text{Cu}_4\text{O}_8$, where $\text{A}:\text{Cu} = 0.75$ (20, 25). Therefore, for $\text{Ba}_{2+y}\text{Cu}_3\text{O}_6$ even for $y = 0$ this ratio (0.67) is the lowest observed and there is no experimental evidence to suggest that it can be reduced any further.

For positive values of y , the “structural integrity” is no longer a concern, and the Ba:Cu content can approach that observed in the other ACuO_2 isomorphs. However, the Ba content will be constrained by the Ba–Ba repulsions within the channels. An estimate of a reasonable minimum Ba–Ba separation can be made by considering typical distances that have been observed in other barium-based cuprates. For example, in $\text{YBa}_2\text{Cu}_3\text{O}_{7-x}$ and $\text{YBa}_2\text{Cu}_4\text{O}_8$ the Ba–Ba distance is approximately equal to the length of the a - and/or b -axes, and lies between 3.8 and 3.9 Å. From the subcell refinements of $\text{Ba}_2\text{Cu}_3\text{O}_6$ presented earlier, the Cu–Cu distance along the cuprate chains is approximately 2.82 Å. Therefore, if the Ba ions in the channels are equally separated, a 3.85 Å Ba–Ba separation would have $\text{Ba}:\text{Cu} = 2.82/3.85 = 0.73$; for $\text{Ba}_{2+y}\text{Cu}_3\text{O}_6$ this corresponds to $y = 0.19$.

By combining reactions [1] and [2], where $\{(3y/4)/[1 + y/2] = x/2\}$, the weight losses calculated for $\text{Ba}_2\text{Cu}_3\text{O}_{6-x}$ can be reinterpreted in terms of the formation of $\text{Ba}_{2+y}\text{Cu}_3\text{O}_6$ to estimate the possible range of y . For example, the weight loss observed prior to the onset of complete phase decomposition corresponded to the formation of $\text{Ba}_2\text{Cu}_3\text{O}_{5.72}$ ($x = 0.28$); using reaction [2], this yields a stoichiometry $\text{Ba}_{2.21}\text{Cu}_3\text{O}_6$ ($y = 0.21$). For the samples prepared directly under reducing conditions, the lowest oxygen content gauged by reaction [2] was $x = 0.38$; in

the new model this is equivalent to $\text{Ba}_{2.29}\text{Cu}_3\text{O}_6$ ($y = 0.29$). Both results are close to the reasonable range of y proposed above.

Additional support for this reduction reaction model can be found in published studies of samples synthesized under high oxygen pressures. In their phase analysis of the Ba–Cu–O system, Williams *et al.* (12) used microprobe techniques to examine the Ba : Cu content of samples prepared from BaO_2 and CuO with initial Ba : Cu ratios ranging from 1:4 to 1:1. In addition to identifying second phases that were consistent with the formation of a compound with a Ba : Cu ratio close to 2:3, these analyses showed the Ba : Cu contents in the primary $\text{Ba}_2\text{Cu}_3\text{O}_{6-x}$ phases ranged from 2:3 to 2:2.7. Using the formulation proposed above, the latter sample corresponds to $\text{Ba}_{2.22}\text{Cu}_3\text{O}_6$, which again is in good agreement with the range of y proposed above.

Further support for the model comes from the studies of the closely related $\text{Ca}_{1-x}\text{CuO}_2$ and $\text{RE}_{2-x}\text{Ca}_{2+x}\text{Cu}_5\text{O}_{10}$ phases. In their structural investigations of calcium cuprate, Milat *et al.* (24) concluded that $\text{Ca}_{5+x}\text{Cu}_6\text{O}_{12}$ can exist over a range of x and that the supercell repeat along the chain direction, i.e., the positions of the diffraction peaks originating from the superstructure, is a function of x and can have commensurate and incommensurate values. Variable ranges of stoichiometry and associated systematic changes in the supercell periodicity were also observed by Davies (20) for the ternary, NaCuO_2 -type, rare earth–Ca cuprates. The results of both studies are consistent with the observations reported here for $\text{Ba}_{2+y}\text{Cu}_3\text{O}_6$.

From the reaction proposed in Eq. [1], it is apparent that the reduction of $\text{Ba}_2\text{Cu}_3\text{O}_6$ to $\text{Ba}_{2+y}\text{Cu}_3\text{O}_6$ should be accompanied by the ex-solution of small amounts of CuO . For the samples prepared from the freeze-dried precursors under reduced p_{O_2} 's no conclusive evidence for the formation of CuO can be found in the X-ray patterns presented in Fig. 7. However, the anticipated amounts of CuO are close to the threshold of detection by X-ray diffraction and the quality of the diffraction patterns for these samples is severely compromised by the small grain size and poor crystallinity arising from the very low synthesis temperature.

Direct evidence for the formation of CuO was also sought by annealing portions of a sample of $\text{Ba}_2\text{Cu}_3\text{O}_6$ prepared at 620°C and 1 atm of oxygen, at 710, 777, and 810°C for 48 h under flowing oxygen. The X-ray patterns collected after each heat treatment are shown in Figs. 8a–8d together with expanded views of the higher angle regions in Fig. 9. In addition to the broadening of several reflections (·) and the appearance of a shoulder on the main peak (arrowed in 8b–8d), the samples annealed at 710°C (Fig. 8b) do show evidence for the formation of small amounts of CuO (×). The continued formation of CuO and broadening and splitting of several

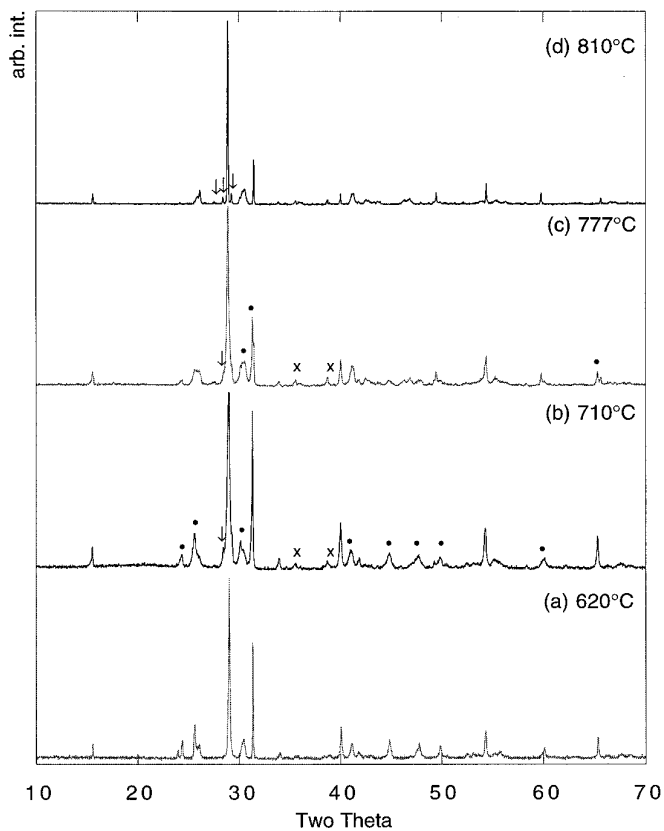


FIG. 8. X-ray patterns of $\text{Ba}_2\text{Cu}_3\text{O}_6$ after annealing for 48 h at (a) 620°C , (b) 710°C (c) 777°C , and (d) 810°C . CuO is indicated by (×), peak broadening by (·), and BaCuO_2 by arrows.

additional reflections is also visible in the patterns of the 777°C (Fig. 8c) and 810°C (Fig. 8d) samples. While the appearance of excess CuO does support the formation of $\text{Ba}_{2+y}\text{Cu}_3\text{O}_6$ with $y > 0$, the peak broadening and splitting in Figs. 8 and 9 seem to be consistent with the evolution of a structure with a discrete value of y rather than a continuous change in the Ba content with temperature. The formation of a high-temperature form of $\text{Ba}_{2+y}\text{Cu}_3\text{O}_6$, possibly a high- y end-member, is similar to the observations of the “high $\text{Ba}_2\text{Cu}_3\text{O}_6$ ” made by Thompson *et al.* (10).

Finally, it must be noted that although the heat treatments of $\text{Ba}_2\text{Cu}_3\text{O}_6$ tend to support the formation of $\text{Ba}_{2+y}\text{Cu}_3\text{O}_6$, many of the changes induced by these heat treatments are impeded by kinetic factors. For example, the shoulder reflections noted above (arrowed in Figs. 8b–8d) originate from the formation of small quantities of BaCuO_2 , and the multiple phases observed in the patterns after the 810°C anneal clearly do not correspond to an equilibrium phase assemblage. Additional experiments (30) in which samples of a 1:1 freeze-dried precursor were reacted directly at temperatures ranging from 650 to 850°C

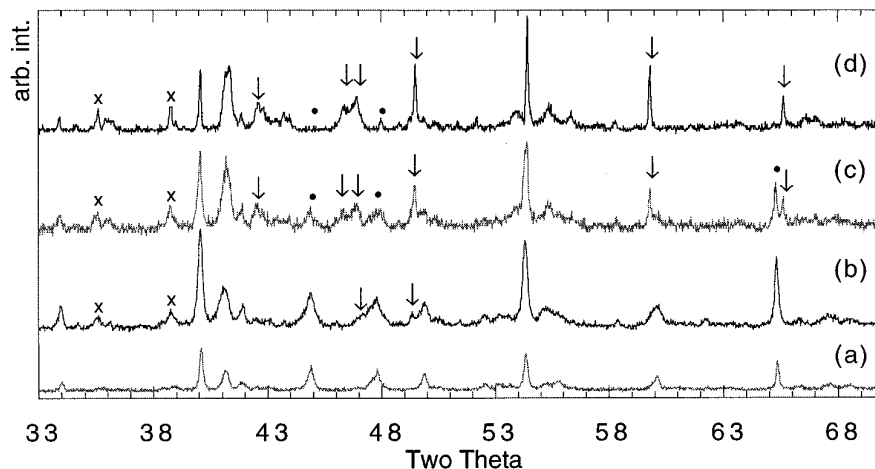


FIG. 9. Expanded view of X-ray patterns in Fig. 9: (a) 620°C, (b) 710°C (c) 777°C, and (d) 810°C. CuO is indicated by (x), peaks evolving from $\text{Ba}_{2+y}\text{Cu}_3\text{O}_6$ by (\downarrow), and disappearing peaks from $\text{Ba}_2\text{Cu}_3\text{O}_6$ by (\bullet).

for several days, indicated that the equilibrium upper stability limit of $\text{Ba}_{2+y}\text{Cu}_3\text{O}_6$ is, in fact, close to 710°C and above this temperature it is unstable with respect to BaCuO_2 .

IV. CONCLUSIONS

Using highly reactive, freeze-dried nitrate precursors it has been demonstrated that $\text{Ba}_2\text{Cu}_3\text{O}_6$ is a stable phase in the Ba–Cu–O system at temperatures below 710°C in 1 atm of oxygen. Reactions of precursors with a 1:1 Ba:Cu stoichiometry yielded a two-phase mixture of $\text{BaO}_2 + \text{Ba}_2\text{Cu}_3\text{O}_6$; no evidence was found for formation of a $\text{BaCuO}_{2.5}$ phase that has been reported in the literature. Investigations of the crystal chemistry of $\text{Ba}_2\text{Cu}_3\text{O}_6$, suggest that it crystallizes in a $\text{KCuO}_2/\text{NaCuO}_2$ -type structure with a Cu sublattice comprised of linear chains of edge-shared, square planar cuprate groups that are cross-linked by Ba ions arranged on a C-centered orthorhombic sublattice. The structure can be stabilized with a lower Cu valence either through preparations under reduced oxygen pressures or by heating $\text{Ba}_2\text{Cu}_3\text{O}_6$ above 620°C. The reduction of copper is accommodated by small increases in the Ba:Cu stoichiometry and formation of $\text{Ba}_{2+y}\text{Cu}_3\text{O}_6$ with y ranging from 0 to approximately 0.25. It is proposed that the reduction in the Ba–Ba repeat distance in the phases with $y > 0$ is responsible for the change in the modulations of the structure that have been reported previously. The formation of small amounts of second-phase CuO in heat treated samples of $\text{Ba}_2\text{Cu}_3\text{O}_6$ provides additional supportive evidence for this reduction mechanism, though the X-ray patterns point to the evolution of a structure with a discrete value of y rather than a continuous change in the Ba content with temperature.

Although reflections from the $\text{Ba}_{2+y}\text{Cu}_3\text{O}_6$ structure persist in samples heated to $T > 800^\circ\text{C}$, longer-term heat treatments indicate it is unstable with respect to BaCuO_2 above 710°C.

ACKNOWLEDGMENTS

This work was supported in part by a grant from the National Science Foundation (DMR 92-00800) and from ITT Defense, GE Aerospace, and the Commonwealth of Pennsylvania through the Ben Franklin Superconductivity Center.

Note added in proof. Recent studies of the Sr–Cu–O system between 600 and 850°C under oxygen pressures up to 600 bar have led to the characterization of a new phase, $\text{Sr}_{0.74}\text{CuO}_2$ (31). Using X-ray and electron diffraction, this compound was found to have Vernier structure related to that of $\text{Ca}_{0.82}\text{CuO}_2$ and NaCuO_2 . The Sr:Cu content and volume of the NaCuO_2 -type subcell in $\text{Sr}_{0.74}\text{CuO}_2$ lie between those for $\text{Ba}_{2+y}\text{Cu}_3\text{O}_6$ and $\text{Ca}_{0.82}\text{CuO}_2$. This work provides further support for the existence of an entire family of alkaline earth “ ACuO_2 -type” cuprates.

REFERENCES

1. E. L. Brosha, E. Sanchez, P. K. Davies, N. V. Coppa, A. Thomas, and R. Salomon, *Physica C* **184**, 353 (1991).
2. E. L. Brosha, P. K. Davies, F. H. Garzon, and I. D. Raistrick, *Science* **260**, 196 (1993).
3. R. Beyers and B. T. Ahn, *Annu. Rev. Mater. Sci.* **21**, 335 (1991).
4. L. R. Morss, S. E. Dorris, T. B. Lindemer, and N. Naito, *Eur. J. Solid State Inorg. Chem.* **27**, 327 (1990).
5. F. H. Garzon, I. D. Raistrick, D. S. Ginley, and J. W. Halloran, *J. Mater. Res.* **6**, 885 (1991).
6. F. H. Garzon and I. D. Raistrick, in “Proceedings of the International Conference on the Chemistry of Electronic Ceramic Materials” (P. K. Davies and R. Roth, Eds.), NIST Spec. Publ., Vol. 804, p. 373. National Institute of Standards and Technology, Gaithersburg, MD, 1990.
7. A. Navrotsky, in “Proceedings of the International Conference on the Chemistry of Electronic Ceramic Materials” (P. K. Davies and

- R. Roth, Eds.), NIST Spec. Publ., Vol. 804, p. 379. National Institute of Standards and Technology, Gaithersburg, MD, 1990.
8. Z. Zhou and A. Navrotsky, *J. Mater. Res.* **7**, 2920 (1992).
 9. J. G. Thompson, J. D. Fitz Gerald, R. L. Withers, P. J. Barlow, and J. S. Anderson, *Mater. Res. Bull.* **24**, 505 (1989).
 10. J. G. Thompson, T. J. White, R. L. Withers, J. D. Fitz Gerald, P. J. Barlow, and S. J. Collocott, *Mater. Forum* **14**, 27 (1990).
 11. I. Halasz, V. Fulop, I. Kirschner, and T. Porjesz, *J. Cryst. Growth* **91**, 444 (1988).
 12. R. K. Williams, K. B. Alexander, J. Brynstad, T. J. Henson, D. M. Kroeger, T. B. Lindemer, G. C. Marsh, J. O. Scarbrough, and E. D. Specht, *J. Appl. Phys.* **70**, 906 (1991).
 13. R. S. Roth, in "Proceedings of User Aspects of Phase Equilibria," p. 25. Joint Research Centre, Petten, The Netherlands, 1990.
 14. G. F. Veronin and S. A. Degterov, *J. Solid State Chem.* **110**, 50 (1994).
 15. M. Arjomand and D. J. Machin, *J. Chem. Soc. Dalton Trans.* **11**, 1061 (1975).
 16. M. Machida, K. Yasuoka, K. Eguchi, and H. Arai, *J. Solid State Chem.* **81**, 176 (1991).
 17. S. Petricek, N. Bukovec, and P. Bukovec, *J. Solid State Chem.* **99**, 58 (1992).
 18. W. Mingmei, S. Qiang, H. Gang, R. Yufang, and W. Hongyang, *J. Solid State Chem.* **110**, 389 (1994).
 19. H. Müller-Buschbaum, *Angew. Chem. Int. Ed. Engl.* **16**, 674 (1977).
 20. P. K. Davies, *J. Solid State Chem.* **95**, 365 (1991).
 21. T. Siegrist, R. S. Roth, C. J. Rawn, and J. J. Ritter, *Chem. Mater.* **2**, 192 (1990).
 22. N. E. Brese, M. O'Keeffe, R. B. Von Dreele, V. G. Young, *J. Solid State Chem.* **83**, 1 (1989).
 23. J. Pickardt, W. Paulus, M. Schmalz and R. Schollhorn, *J. Solid State Chem.* **89**, 308 (1990).
 24. O. Milat, G. Van Tendeloo, S. Amelinckx, T. G. N. Babu, and C. Greaves, *J. Solid State Chem.* **101**, 92 (1992).
 25. P. K. Davies, E. Caignol, and T. King, *J. Am. Ceram. Soc.* **74**, 569 (1991).
 26. K. Hestermann and R. Hoppe, *Z. Anorg. Allg. Chem.* **367**, 249 (1969).
 27. K. Wahl and W. Klemm, *Z. Anorg. Allg. Chem.* **270**, 69 (1952).
 28. H. D. Wasel-Nielen and R. Hoppe, *Z. Anorg. Allg. Chem.* **375**, 43 (1970).
 29. R. S. Roth, K. L. Davis, and J. R. Dennis, *Adv. Ceram. Mater.* **2**, 303 (1987).
 30. E. L. Brosha, F. H. Garzon, I. D. Raistrick, and P. K. Davies, *J. Am. Ceram. Soc.* **78**, 1745 (1995).
 31. P. V. P. S. S. Sastry, A. D. Robertson, E. E. Lachowski, A. Coats, and A. R. West, *J. Mater. Chem.* **5**(11), 1931 (1995).